# RELATIVISTIC ELECTRON BEAM TRACKING OF REDUCED DENSITY CHANNELS IN NORMAL DENSITY AIR

D. Murphy, R. Pechacek, J. Antoniades[a], T. Peyser[b], M. Myers, R. Fernsler, R. Hubbard, and R. Meger
Charged Particle Physics Branch-----Plasma Physics Division
Naval Research Laboratory-----Washington, DC 20375-5000

## Abstract

A high-current relativistic electron beam injected into a uniform background gas will drive a significant return current in the beam induced background plasma. Interaction of the return current with the beam current can drive the beam off axis, possibly resulting in a disruptive beam instability such as the resistive hose. If the beam is injected into a cylindrical, reduced-density channel in normal density air, the return current will preferentially flow in the higher density edges of the channel. The dipole component of this return current distribution will produce a net centering or tracking force on the beam causing it to follow the density channel. This mechanism would provide a means of guiding a beam to a desired target as well as minimizing scattering and energy loss along the way. Preliminary results indicate that at least the first half of the SuperIBEX electron beam pulse has been seen to track the density channel.

## Introduction

The goal of this research is to experimentally test two predicted effects of the interaction between electron beams and neutral, reduced-density channels. First the theory suggests that a positive tracking force exists between a density channel and an electron beam arising from asymmetric plasma current flow induced by the beam in the channel. This prediction was verified a few years ago over short distances using low current, low $\gamma$ beams and channels offset from the propagation chamber axis[1,2] and has been retested recently using higher $\gamma$ beams. Secondly if the beam stays in the channel (Beam in Channel Propagation Mode) for a significant distance then the rate of radius expansion of the beam due to scattering on air molecules (Nordsieck Expansion) will decrease below that for a beam propagating in full density air (Lead Pulse Propagation Mode).

## Hardware

### Production

The SuperIBEX diode uses an unmagnetized, cold-cathode arrangement. At present the beam is extracted through a thin anode foil and aperture and injected directly into a 40cm long by 10cm diameter, low

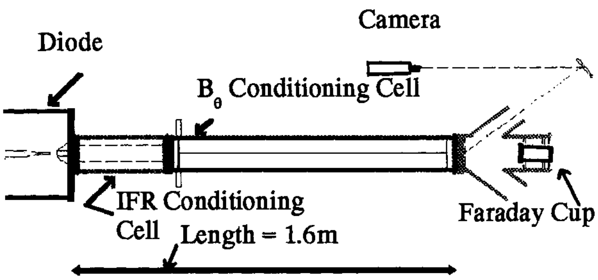


Figure 1 Beam Generation Hardware

pressure IFR conditioning cell.(See Figure 1.) A 1.5mil titanium exit foil separates the IFR cell from the adjacent atmospheric pressure $B_\theta$ cell. The IFR cell with its 1.5mil thick exit foil produces the required radius tailoring while the 1.3m long by 20cm diameter $B_\theta$ cell provides beam centering and damping of inherent beam sweep while adding some additional heating to the beam. The cell uses a single, on-axis, 21mil diameter copper wire supported by cross hairs at each end and pulsed to 9kA to provide the axially uniform, $\Theta$-magnetic field which guides the beam. Previously, the beam was injected from the diode into a passive two-stage, IFR cell which had to both center and radius tailor the beam. This passive structure was used for the initial off-axis channel tracking studies.

A 1/4mil thick, aluminized mylar foil separates the conditioning hardware from the propagation chamber and provides an electrical ground for the Laser Guided Electric Discharge (LGED) which produces the channel. A diagnostics cell containing a Teflon Cerenkov foil and a segmented Faraday cup can be mounted at the end of the conditioning cell. Table I shows the beam characteristics at each stage in its generation.

Table I

| SuperIBEX Beam Characteristics | Diode Only | Diode With Single IFR Tailoring Cell | Diode With Passive, Two-Stage IFR Cell | Diode With IFR Cell and $B_\theta$ Cell |
|---|---|---|---|---|
| Peak Voltage | 5.3MV | 5.3MV | 5.3MV | 5.3MV |
| Peak Current | 27kA | 24kA | 8kA | 16kA |
| FWHM | 30ns | 28ns | 28ns | 25ns |
| Beam Radius | 0.6cm | 1.2cm | 2.0cm | 1.6cm |
| Tailoring | None | 4:1 | 3:1 | 4:1 |
| Stability | Poor | Fair | Good | Excellent |

### Propagation and Diagnostics

As the beam emerges from the 1.3m long by 20cm diameter $B_\theta$ cell it enters a 1.3m long by 60cm diameter section of propagation chamber. (See Figure 2.) The first set of net-current, B-dot probes are mounted in the chamber wall just before the transition into the 5m long by 2m diameter section of propagation chamber. In the larger chamber B-dot probes are mounted on long stalks which project in to a radius of 50cm. Sets of 4 probes are spaced at 0.5m or 1m intervals down the axis of this section. The signals from each 4-probe set are numerically processed to yield the net current and the net current centroid position vs time. Many ports provide optical access to this section also. Camera types include open-shutter film cameras, a film loaded streak camera, and gated microchannel video cameras.

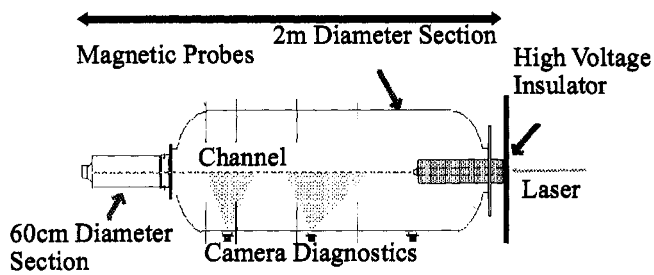


Figure 2 Beam Propagation Chamber

### Channel Production

The reduced-density channels are produced by the technique of Laser Guided Electric Discharges (LGED).[3] At the end of the propagation chamber is an insulated, hollow high-voltage electrode. The laser preionizes a path between this electrode and a thin aluminized mylar foil covering the entrance aperture, up to 5.2m away. At the same time a 1.5MV marx generator is pulsed on to break down the preionized path. An inductively isolated (160μH) auxiliary capacitor bank (20μF, 30kV) is connected in parallel with the marx bank which adds additional energy to the discharge in order to make a larger diameter, deeper channel. These channels expand rapidly to pressure equilibrium at ~3cm radius and then grow more slowly to ~5cm radius while cooling. Their central density is initially about 0.1 atmosphere but they gradually fill in as turbulent convective mixing pushes cold,

# Report Documentation Page

*Form Approved*
*OMB No. 0704-0188*



| 1. REPORT DATE | 2. REPORT TYPE | 3. DATES COVERED |
|---|---|---|
| **JUN 1991** | **N/A** | **-** |

4. TITLE AND SUBTITLE
**Relativistic Electron Beam Tracking Of Reduced Density Channels In Normal Density Air**

5a. CONTRACT NUMBER
5b. GRANT NUMBER
5c. PROGRAM ELEMENT NUMBER

6. AUTHOR(S)

5d. PROJECT NUMBER
5e. TASK NUMBER
5f. WORK UNIT NUMBER

7. PERFORMING ORGANIZATION NAME(S) AND ADDRESS(ES)
**Plasma Physics Division, Naval Research Laboratory, Washington, D.C. 20375-5000**

8. PERFORMING ORGANIZATION REPORT NUMBER

9. SPONSORING/MONITORING AGENCY NAME(S) AND ADDRESS(ES)

10. SPONSOR/MONITOR'S ACRONYM(S)

11. SPONSOR/MONITOR'S REPORT NUMBER(S)

12. DISTRIBUTION/AVAILABILITY STATEMENT
**Approved for public release, distribution unlimited**

13. SUPPLEMENTARY NOTES
**See also ADM002371. 2013 IEEE Pulsed Power Conference, Digest of Technical Papers 1976-2013, and Abstracts of the 2013 IEEE International Conference on Plasma Science. Held in San Francisco, CA on 16-21 June 2013. U.S. Government or Federal Purpose Rights License.**

14. ABSTRACT
**A high-current relativistic electron beam injected into a uniform background gas will drive a significant return current in the beam induced background plasma. Interaction of the return current with the beam current can drive the beam off axis, possibly resulting in a disruptive beam instability such as the resistive hose. If the beam is injected into a cylindrical, reduced-density channel in normal density air, the return current will preferentially flow in the higher density edges of the channel. The dipole component of this return current distribution will produce a net centering or tracking force on the beam causing it to follow the density channel. This mechanism would provide a means of guiding a beam to a desired target as well as minimizing scattering and energy loss along the way. Preliminary results indicate that at least the first half of the SuperiBEX electron beam pulse has been seen to track the density channel.**

15. SUBJECT TERMS

| 16. SECURITY CLASSIFICATION OF: | | | 17. LIMITATION OF ABSTRACT | 18. NUMBER OF PAGES | 19a. NAME OF RESPONSIBLE PERSON |
|---|---|---|---|---|---|
| a. REPORT | b. ABSTRACT | c. THIS PAGE | | | |
| **unclassified** | **unclassified** | **unclassified** | **SAR** | **4** | |

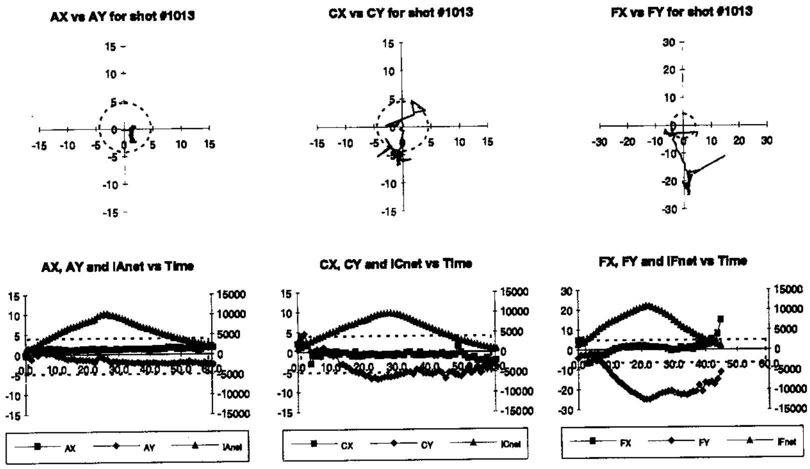


Figure 6 Propagation Without A Channel Shot# 1013

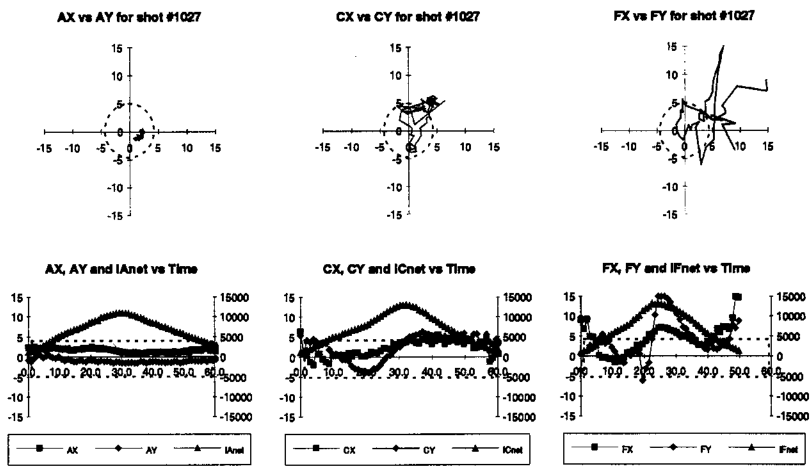


Figure 7 Propagation Without A Channel Shot# 1027

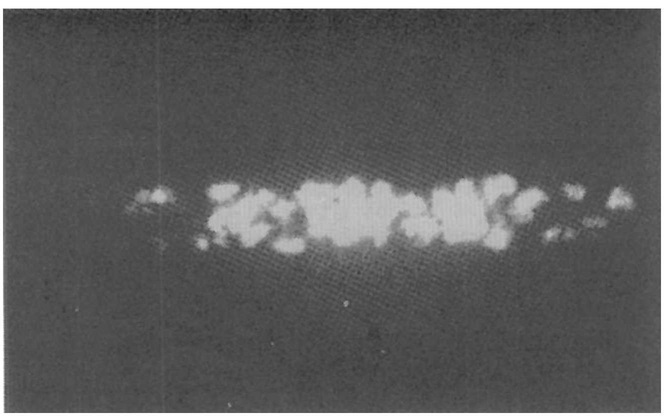

Figure 8 Open Shutter Photograph of Beam and 8ms Old Channel

## Optical Data

The reason for the onset of this hose type instability may be revealed in Figure 8 which is a photograph of a beam injected into an 8ms old channel. The channel is still glowing sufficiently even this long after the discharge heating has ended to nearly obscure the beam induce air fluorescense in and around the channel. The late time granularity of the channel due to turbulent convective mixing is evident in the photograph. The camera shutter was opened at ~7ms and left open. Numerical simulations of the interaction between this beam and a turbulent channel predict a coupling between the channel inhomogeneity and the growth rate of the hose instability.

Figure 9 is a comparison of the beam radius as a function of propagation distance that might be expected for a "Lead Pulse" (No-Channel) beam and a beam in an On-Axis Channel, $L_N$ = 300cm and $L_N$ =500cm respectively. After a couple of meters of propagation the difference between the radii should be apparent even to simple, open-shutter photography. Figure 10 presents two open-shutter photographs of the beam induced air fluorescence showing the difference in the beam diameter without and with a channel present, shots #1025 and #1026 respectively. When no channel is present the scattering of the beam electrons off air molecules is greater than when a reduced-density channel is in the beam line. The time delay between channel initiation and beam injection for the lower photograph is 16ms. After such a long delay the channel would be very shallow so the range extension would not be as large as for a deeper channel.

Figure 11 displays measured beam gaussian radii for these two shots obtained from various sources at Z=0, Z=240cm and Z=410cm for these same two shots. Exponential curves are fitted through the data points to determine a Nordsieck scattering length for each beam. The Nordsieck Length for shot#1025 (16ms delay channel) is ~470cm. The Nordsieck Length for shot#1026 (No-Channel) is ~390cm.

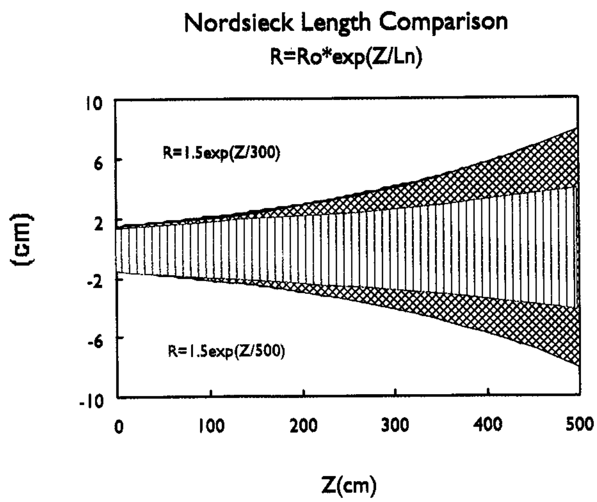


Figure 9 Calculated Rate of Expansion of the Beam Envelope

outside air into the channel. These channels are very long lasting, on the order of a 100 millisecond or more.

### Off-Axis Channel Tracking

Figure 3 shows X vs Y cross-plots and the X, Y, and Inet vs Time plots for a 3.5ms delay, off-axis channel tracking shot, #755. The dotted lines indicate the position of the channel relative to the propagation chamber axis. In this experimental run during the autumn of 1990 with the two-stage IFR centering/conditioning hardware only the A probe set (Z=62cm) and the C probe set (Z=182cm) were active. The tracking force is proportional to the beam current which was relatively low at only 8kA and the beam stability without a channel present was not good beyond Z=2m. The channel was only 3m in length but the same energy per unit length was deposited in the channel as on subsequent experiments with longer channels. We found that only the head of the beam tended to track toward the channel. Just at or near the peak of the current pulse the beam tended to leave the channel. Due to the poor quality of the beam produced by the two-stage IFR apparatus a development effort was undertaken to produce a beam with higher current and stable propagation characteristics. This effort led to the IFR/Bθ cell configuration.

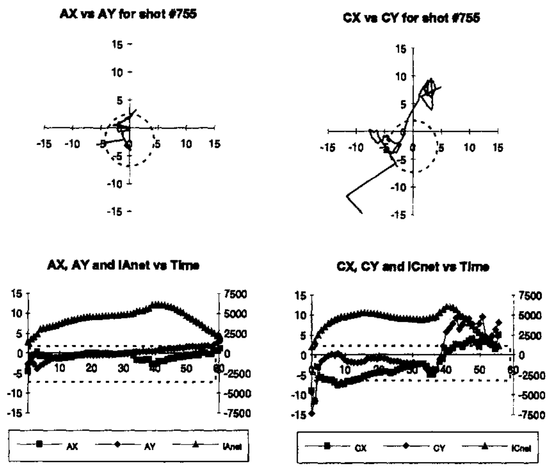


Figure 3. Tracking of an Off-Axis Channel

### Lead Pulse (No-Channel) Propagation

#### Magnetic Probe Data

Figure 4 shows the time averaged beam position (X,Y) and standard deviation ($\sigma_x, \sigma_y$) at three Z positions for nine No-Channel shots using the IFR/Bθ hardware. Magnetic probe set A is at Z=1.3m, the C set at Z=2.5m, and the F set at 4.5m. There is a residual, low frequency motion in the net current centroid of the order of ~5cm at Z=4.5m that the conditioning apparatus was not able to remove. The initial beam radius is ~1.6cm and in full density air this beam has a calculated Nordsieck scattering length of $L_N$ ~ 4m so the beam radius at Z=4.5m should be ~5cm, thus this motion is still only on the order of one beam radius.

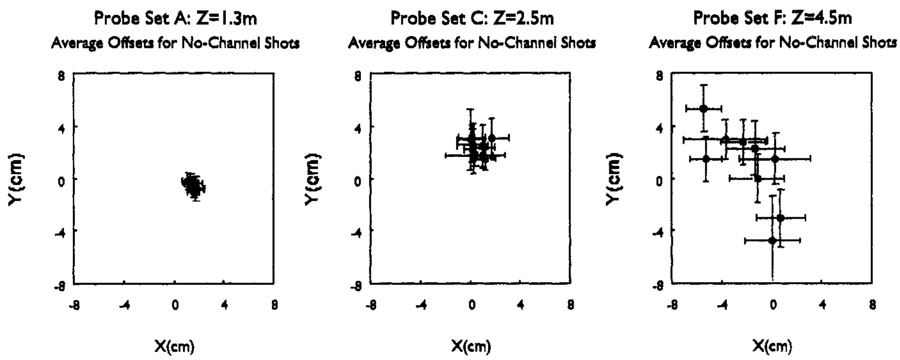


Figure 4 Net Current Centroid Motion For No-Channel Shots

Figure 5 shows X vs Y cross-plots and the X, Y, and Inet vs Time plots for a typical No-Channel shot, #1020 which was included in the data set shown in Figure 4. It further emphasizes that while the beam may drift slightly off axis the high frequency hose motion is still quite small. Much of the apparent fluctuation in the centroid position very late in the pulse is due to numerical errors related to division by small values of the total net current.

### On-Axis Channel Propagation

#### Magnetic Probe Data

Figure 6 shows X vs Y cross-plots and the X, Y, and Inet vs Time plots for shot #1013, a 4ms channel delay shot. It shows an essentially monotonically increasing offset of the beam as a function of both the propagation distance and the pulse time. This is an example of Beam into Channel injection wherein the channel conductivity is too high at injection time. The channel undergoes avalanche ionization resulting in a return current distribution that ejects the beam from the channel. Figure 7 shows X vs Y cross-plots and the X, Y, and Inet vs Time plots for shot #1027, an 8ms channel delay shot. It shows an unexpectedly strong hose motion which grows as the beam propagates down the target chamber. While the beam was relatively stable through the A probe set position, Z=1.3m, the beam became increasing unstable the further it propagated.

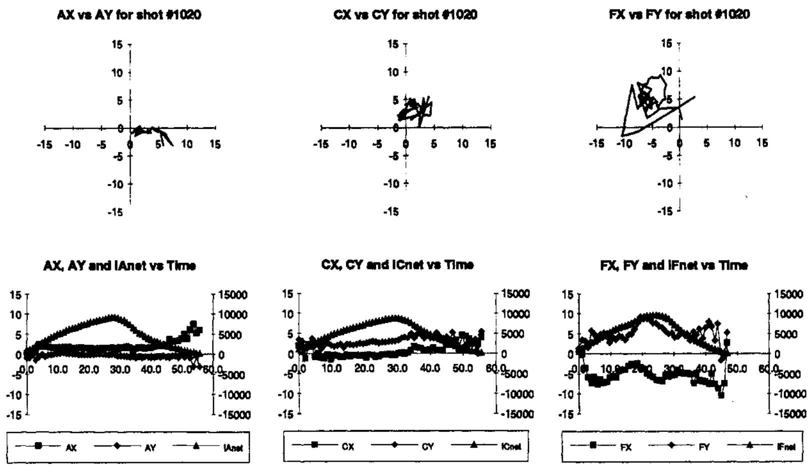


Figure 5 Propagation Without A Channel Shot# 1020

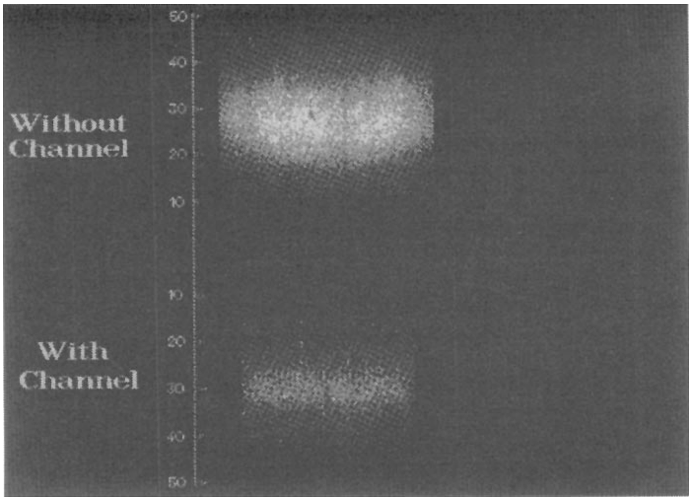


Figure 10 Open Shutter Photographs of Shots 1025 and 1026

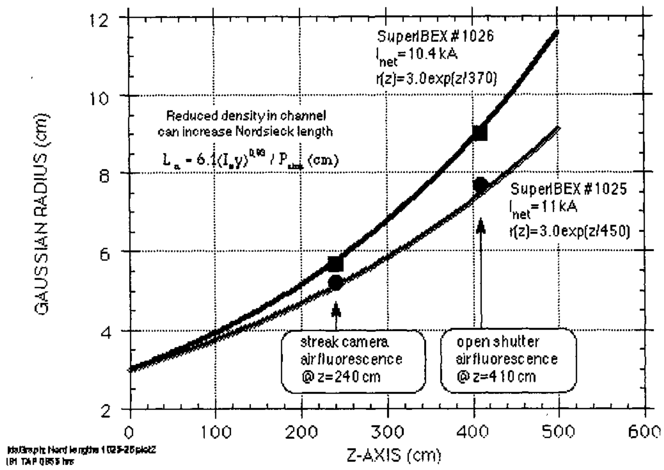


Figure 11 Analysis of Beam Expansion for Shots 1025 and 1026

## Conclusions

In the initial data run to test offset channel tracking with high $\gamma$ beams there was evidence that at least the first half of the beam did track the channel before being ejected. However the beam was low current and inherently hose unstable making it unsuitable for continued offset channel tests. After a development program on the conditioning cells we were able to produce high current stable beams. A second data run was completed this spring using stable beams for injection into the reduced-density channels. As expected the beam is expelled from the channel if the residual conductivity of the channel is not allowed to decay before beam injection. These beams experienced unexpectedly large hose oscillations when injected into what are deemed low conductivity channels. Numerical simulations indicate that the instablility may be driven by a coupling between the beam and large scale density fluctuations in the channel caused by turbulent convective mixing of cold normal density air into the hot reduced density channel. Using optical measurements we were able to verify that the scattering length did increase when the beam stayed in the channel even though the channel on shot#1025 was very shallow (16ms delay).

Work supported by DARPA, ARPA order 7781, and ONR.
aSachs-Freeman Associates,Landover, Md.
bScience Applications International Corp., Mclean, Va

## References

[1]Density Channel Tracking Studies on Pulserad, D.P. Murphy, R.E. Pechacek, R.F. Fernsler, D.P. Taggart,and R.A. Meger, NRL Memo Report 6770, March 2, 1991.
[2]D.R. Welch, F.M. Bieniosek and B.B. Godfrey, Phys. Rev. Lett., 65, 3128 (1990).
[3]J.R. Greig, et. al., Proc. 7th Int. Conf. on Gas Discharges, (London, 1982) and D.P. Murphy, et. al., NRL Memo Report 5688, Feb 1986.